УДК 539.421

Угол раскрытия вершины трещины как параметр сопротивления разрушению в описании распространения и остановки вязких трещин в стальных трубах в условиях рабочего давления

M. Ben Amara[1], G. Pluvinage[2], J. Capelle[1], Z. Azari[1]

[1] Национальная школа инженеров Меца, Мец, 57078, Франция
[2] Fiabilité Mécanique Conseils, Сийи-сюр-Нье, 57530, Франция

Угол между двумя сторонами элемента, представляющий собой вершину трещины, называется углом раскрытия вершины трещины. Его критическая величина используется в качестве критерия сопротивления разрушению при описании устойчивой трещины отрыва в тонких металлических материалах. Для определения угла раскрытия вершины трещины применяются различные методы. К наиболее распространенным методам относятся оптическая микроскопия и сглаживание экспериментальных кривых зависимости смещений от нагрузки с помощью метода конечных элементов (метод корреляции цифровых изображений). Также применяется аналитический анализ с использованием экспериментальных диаграмм «смещение – нагрузка» (метод одного образца), разработанный на основе модели пластического шарнира при трехточечном изгибе вязкого образца. В рамках данного подхода расстояние до центра поворота считается постоянным. В настоящей работе приведены значения угла раскрытия вершины трещины для трубопроводной стали марки API 5L X65, вычисленные с использованием трех методов: метод корреляции цифровых изображений, комбинированный численный метод и упрощенный метод одного образца. Полученные значения угла раскрытия близки между собой и примерно равны 20°. Обсуждаются различные параметры, характеризующие сопротивление росту трещин в трубах в условиях рабочего давления. Рассмотрены энергия разрушения при ударной нагрузке, определяемая в испытаниях по Шарпи или ударных испытаниях на разрыв, критическая энергия J, кривая текучести после разрушения, энергия в зоне сцепления, а также угол раскрытия вершины трещины. Значение данного угла считается неизменным в случае устойчивого роста трещины, но уменьшается линейно в соответствии с ростом трещины на начальном этапе ее неустойчивого развития. Представлена численная процедура описания вязкой растущей трещины на основе метода удаления узлов, в котором угол раскрытия вершины трещины используется в качестве критерия сопротивления разрушению. Проведено сравнение предлагаемого метода с тремя другими методами двух кривых: метод Бателли, метод высокопрочных труб и метод Sumitomo для высокопрочных труб. Оценка по методу Бателли, основанному на ударной вязкости по Шарпи, крайне консервативна. Оценка по методу угла раскрытия вершины трещины близка к прогнозу по методу Sumitomo для высокопрочных труб.

Ключевые слова: распространение вязких трещин, труба, угол раскрытия вершины трещины, сталь

Crack tip opening angle as a fracture resistance parameter to describe ductile crack extension and arrest in steel pipes under service pressure

M. Ben Amara[1], G. Pluvinage[2], J. Capelle[1], and Z. Azari[1]

[1] Laboratoire de Mécanique Biomécanique Polymère Structures, École Nationale d'Ingénieurs de Metz, Metz, 57078, France
[2] Fiabilité Mécanique Conseils, Silly sur Nied, 57530, France

The angle between two element sides representing the crack tip is defined as the crack tip opening angle (CTOA). Its critical value is used as a criterion of fracture resistance for characterizing stable tearing in thin metallic materials. Various methods are used for determination of the CTOA. Optical microscopy is one of the most common methods as well as fitting of experimental load–displacement diagrams by the finite element method (DIC). Additionally, analytical analysis using the experimental load–displacement curve method (SSM) derived from the plastic hinge model of deflection in three-point bending of a ductile specimen is applied. This approach assumes a constant rotation centre distance. Values of CTOA for API 5L X65 pipe steel found by three methods—DIC, CNM, and SSM—are given. Values of CTOA given by these three methods are similar and close to 20°. A discussion on the different parameters used to characterize the fracture resistance of running cracks in a pipe under service pressure is presented. The energy of fracture at impact determined by Charpy or drop-weight tear test (DWTT) tests and the critical J energy parameter are considered as well as the yield locus after damage, cohesive zone energy, and CTOA is another approach. One notes that CTOA is assumed to be constant during stable crack extension and decreases linearly with crack length during the instable and primary phase. A numerical technique to describe a ductile running crack using the node release technique and using CTOA as the fracture resistance criterion is presented. This method is compared with three different two-curve methods (TCMs): the Battelle, high strength line pipe (HLP), and HLP-Sumitomo methods. The Batelle TCM, as the oldest method, based on Charpy energy, gives a strongly conservative prediction. Predictions by the CTOA method are close to those obtained by the HLP-Sumitomo one.

Keywords: ductile crack extension, pipe, crack tip opening angle (CTOA), steel

© Ben Amara M., Pluvinage G., Capelle J., and Azari Z., 2015

1. Introduction

The concept of crack tip opening angle (CTOA) was probably introduced by Anderson in 1972 [1] to simulate stable crack growth by the finite element method. In this method, crack growth is obtained by successive relaxation of the nodal forces at the node representing the crack tip. The ψ angle between two element sides representing the crack tip was chosen as the criterion for the crack growth. However, crack growth dependence of this angle was expected, and a constant value was used for all of the stages of growth. The value at the first increment of crack growth called ψ_0 was determined from the experimentally determined critical value of the *J* integral. Anderson assumed that after large crack growth, steady state conditions prevail and ψ stabilizes to the ψ_{stab} value with $\psi_{stab} < \psi_0$. Rice [2] has pointed out the difficulty of using this parameter for the simulation of crack growth in an elastic-plastic material. In this case, displacement exhibits a profile proportional to the product *r* (where *r* is the distance measured from the crack tip). Therefore the tangent at the crack tip corresponds to an ambiguous definition of the CTOA.

Several authors [3–6] using two dimensional analysis showed that CTOA at initiation is always larger than the value at stable crack growth (Fig. 1).

One of the first experimental determinations of the CTOA was mentioned by Luxmoore et al. [7]. Using centre notched and double-edge notched specimens of aluminium alloy, they measured the CTOA during stable crack growth. They noted that the crack tip opening δ varied linearly with increases in crack length. This linear behaviour indicated that the CTOA remains constant and equal to 2.1°. This was also previously noticed by de Koning et al. [8].

Conditions of stable crack growth require that the rate of change of the crack driving force with increasing crack length Δ*a* is smaller than the increase of crack growth resistance expressed in terms of crack opening displacement:

$$\frac{\mathrm{d}\delta}{\mathrm{d}a} \le \frac{\mathrm{d}\delta_R}{\mathrm{d}a}. \tag{1}$$

It can be seen on the *R* curve $\delta_R = f(a)$ that the terms

$$\frac{\mathrm{d}\delta_R}{\mathrm{d}a} = \mathrm{CTOA}, \tag{2}$$

CTOA is constant in the linear part of the *R* curve (Fig. 2).

Early experimental determination of CTOA was carried out by Reuter et al. [9] using microtopography and Dawicke et al. [10] using a high-resolution photographic camera with a video system. Dawicke et al. [10] also compared the high-resolution photographic method and a digital-imaging correlation method to measure the surface CTOA values. These two methods gave very similar CTOA values for thin-sheet aluminium alloys.

During the last decade, extensive studies applying the CTOA concept to ductile fracture have been undertaken. As a result, the CTOA-based fracture mechanics method has become mature, and a standard test method for critical CTOA testing was developed recently by ASTM with the designation E2472-06e1 [11]. The recommended specimens are the compact-tension C(T) and middle-crack-tension M(T) specimens made from thin-sheet materials in order to achieve low constraint conditions at the crack tip. The standard was validated by Heerens and Schodel [12] using a comprehensive dataset on the stable crack extension in an aluminium sheet material with a thickness of 3 mm.

The CTOA fracture criterion has now become one of the most promising fracture criteria used for characterizing stable tearing in thin metallic materials. Initially, fracture resistance to crack extension was given by Charpy energy, as in the Battelle two-curves method (BTCM) [13]. The Charpy test is related to crack initiation, bending of the specimen, and plastic deformation at the load points. It is necessary that tests performed to characterize the propagation resistance be able to isolate and quantify the propagation energy with respect to incremental crack advance. For this reason and due to the development of higher strength steels with increased toughness and lower transition temperatures by using controlled rolling techniques, Charpy energy was replaced by drop-weight tear test (DWTT) energy in the HLP two-curve method [14]. DWTT tests are also related to crack initiation, bending of the specimen, and plastic deformation. However, notched DWTT specimens are larger

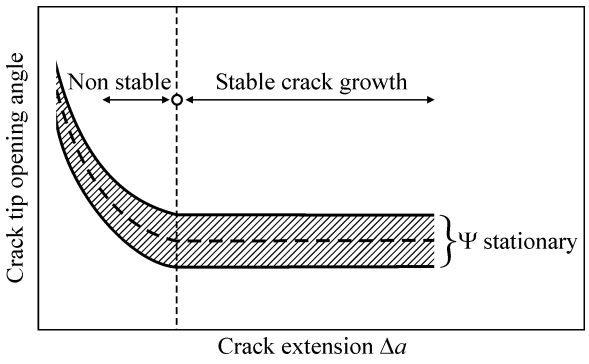


Fig. 1. Evolution of CTOA during crack extension

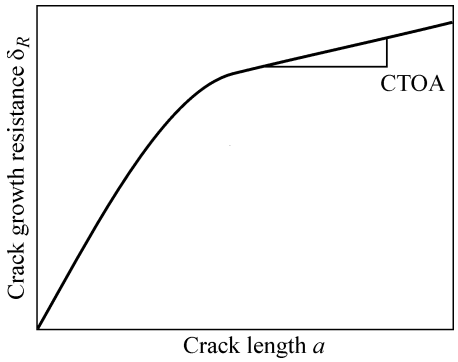


Fig. 2. Definition of CTOA on *R* curve $\delta_R = f(a)$

than Charpy ones and therefore relatively less of the total fracture energy is related to initiation. The statically precracked DWTT showed the best compromise between isolating the propagation energy and ease of specimen preparation. Another step was the development of a test methodology to indirectly measure CTOA, derived on the basis of the difference in energy between two modified DWTT specimens with different initial crack lengths [15].

The use of CTOA for prediction of dynamic ductile fracture arrest in pipelines began in the late 1980s with a model which calculates the crack driving force in terms of CTOA as a function of crack speed.

As a result of the parametric study, an interpolation formula for maximum CTOA has been developed for pipeline steels [16] and is given by the general form

$$\text{CTOA} = C\left(\frac{\sigma_\text{h}}{E}\right)^m\left(\frac{\sigma_\text{h}}{\sigma_0}\right)^n\left(\frac{D}{t}\right)^q, \quad (3)$$

where m, n, and q are dimensionless constants and C is expressed in units of degrees, σ_h is the hoop stress (MPa), σ_0 is the flow stress (MPa), D is the diameter (mm), and t is thickness (mm). The following values can be used for methane: $C = 106$, $m = 0.753$, $n = 0.778$, and $q = 0.65$.

2. Experimental determination of CTOA on API 5L X65 pipe steel

2.1. Definition

The CTOA is defined as the angle between the crack faces of a growing crack. The practical realization of this definition is not possible because the crack faces are not straight but curved with a curvature which depends on the specimen and loading type. A definition based on crack tip opening displacement δ at a distance d of the order of 1 mm is consistent for both experimental and numerical determination (Fig. 3)

$$\Psi = \arctan\left(\frac{\delta}{2d}\right). \quad (4)$$

In order to overcome the zigzag pattern of real crack faces or the influence of mesh size, it is more convenient to determine CTOAs at several distinct complementary positions on the upper and lower crack surfaces Ψ_i, and to average over these values afterwards (Fig. 4). The points used to determine the Ψ_i values should be chosen in the range of 0.5 to 1.5 mm behind the crack tip

$$\Psi = \frac{1}{N_i}\sum_1^{N_i}\Psi_i. \quad (5)$$

2.2. Measurements of CTOA

Various methods are used for experimental determination of the CTOA. These comprise microtopography, optical microscopy, finite element fitting, or analytical analysis of experimental load displacement curves.

In microtopography [17], the fracture surfaces are topographically analysed post-mortem. This method is based on the assumption that the CTOA is preserved in the plastic deformations of the fracture surface. After both surfaces have been scanned, they are recombined in the computer. The reconstructed crack contours at fracture allow the determination of the CTOA. This method is of interest because it allows the CTOA to be identified in positions of different thicknesses, but it is time consuming.

The calculation of the critical CTOA can be made using the dynamic fracture results from two specimens with different notch depths [18]. These specimens are three-point bend specimens similar to the DWTT specimen but with a straight notch machined in the place of the standard pressed notch. Evaluating the fracture energy difference makes it possible to suppress the crack initiation energy and give the propagation energy proportional to ligament area. CTOA is obtained by the following formula:

$$\Psi_\text{c} = \frac{180}{\pi}\frac{C_1 S_\text{c}}{R_\text{c,d}}, \quad (6)$$

where $C_1 = \text{const}$,

$$S_\text{c} = \frac{(E/A)_\text{shallow} - (E/A)_\text{deep}}{28}, \text{J/mm}^2, \quad (7)$$

$(E/A)_\text{shallow}$ is the energy per area for a shallow-notch specimen ($a = 10$ mm, $a/W = 0.13$), $(E/A)_\text{deep}$ is the energy per area for a deep-notch specimen ($a = 38$ mm, $a/W = 0.5$), $R_\text{c,d}$ is the dynamic flow stress ($R_\text{c,d} = R_\text{c,s}$), $R_\text{c,s}$ is the static flow stress, a is the crack length, and W is the specimen width.

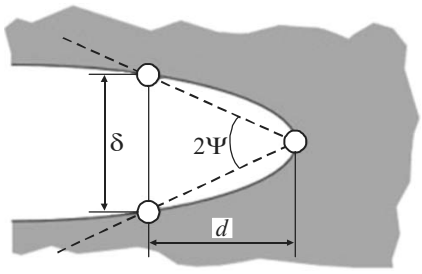


Fig. 3. Definition of CTOA on the curved crack profile

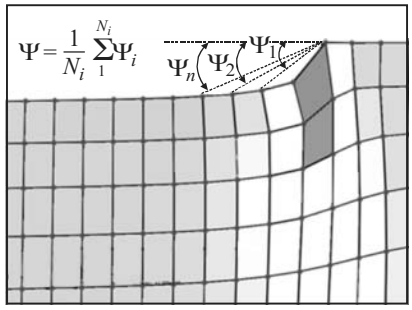


Fig. 4. Definition of CTOA according to the meshing crack

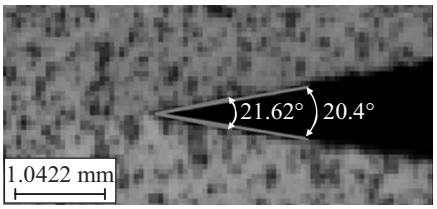


Fig. 5. Digital image of a crack and corresponding CTOA values

Optical microscopy is one of the most common methods of measuring CTOA [18]. The crack contour close to the crack tip is investigated at the polished surface using a light microscope. A special case of optical measurement is the digital image correlation (DIC) method. For our measures, a commercial DIC camera (Gom FASTCAM SA.1 Photron) and a software analysis package with integrated length and angle measurement tools (ARAMIS V6.3) has been used to measure CTOA and crack extension Δa. The recording time was automatically available from the videotapes, where a digital stopwatch was used to synchronize the still images. All of this allowed test parameters such as load, displacement, and crack length Δa are correlated with CTOA. One example of such a digital image and the corresponding CTOA values is given in Fig. 5.

In the finite element fitting of experimental load–displacement diagrams [19], the ones used are the load–Δa or the load–crack opening displacement diagrams. These diagrams are reproduced by finite element analysis using the CTOA as the controlling parameter for crack extension. Evolution of a CTOA with crack extension is obtained numerically and is called the combined numerical method (CNM). To provide a basis for comparison with the DIC method, the measuring distance d behind the crack tip was taken as 0.5 to 1.5 mm. Figure 6 shows the CTOA versus crack extension data obtained from modified CT specimens using the digital correlation camera (DIC) method and CNM. As we observe, the DIC measured data do not exhibit the initial rapid decrease in CTOA; however they are quite comparable to the CTOA measurements obtained using the CNM in the constant CTOA range. Consequently, the second method offers greater advantage in terms of its accuracy as well as its implementation.

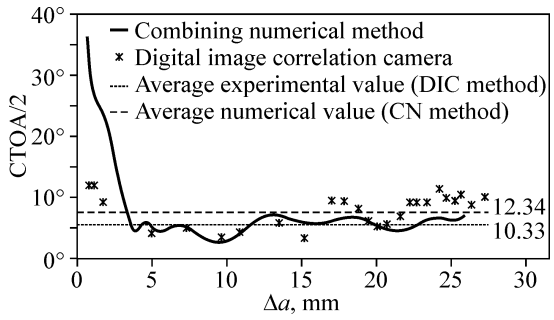


Fig. 6. Comparison of CTOA versus crack extension curve obtained by CNM and the DIC method for a modified CT specimen made of X65 pipe steel

Analytical analysis of experimental load–displacement curves in order to determine the CTOA can be carried out using two different assumptions. The first one considers that the material has the stress strain behaviour of an elastic perfectly plastic material. The second assumptions consider that the material is strain hardening and the stress strain cure is described by a key curve.

Xu et al. [20] developed a method derived from the plastic hinge ductile fracture model [21], called the simplified single-specimen method (SSM). This model employs a regression algorithm of logarithmic load against displacement, avoiding the determination of crack extension and removing the requirements of material-based parameters. It is assumed that the ligament is fully yielded and the specimen rotates around a fixed centre of rotation at a distance of $r^*(W-a) = r^*b$ from the crack tip (Fig. 7), where r^* is the rotation constant. Neglecting the small change in position of the centre of rotation for a small increment of crack length, the half crack-tip opening displacement can be related to a small increment of rotation angle ($d\alpha$) by

$$\frac{\delta}{2} = r^*(W-a)d\alpha. \tag{8}$$

From these relations, CTOA can be written as

$$\tan\left(\frac{\Psi}{2}\right) = r^*b\frac{d\alpha}{dy}. \tag{9}$$

Assuming that the material has a perfectly plastic behaviour, the limit moment M_L of a three-point bending (3PB) specimen is given by

$$M_L = \frac{P_L S}{4}, \tag{10}$$

where P_L is the limit load and S is the span. The limit load is given by

$$P_L = \frac{4AR_cBb^2}{S}, \tag{11}$$

where A is a geometrical constant which depends on the stress state, R_c is the flow stress, b is the ligament, and B is the thickness. During the crack extension increment Δa, the limit load decreases by ΔP_L, the specimen arms rotate by

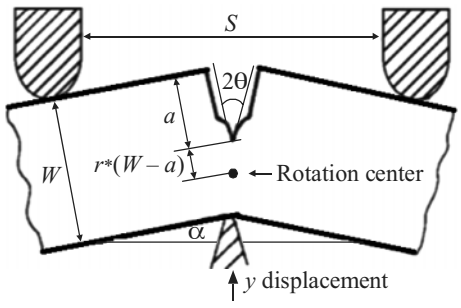


Fig. 7. Mechanisms of plastic deformation of a 3PB specimen assuming the existence of a rotation centre

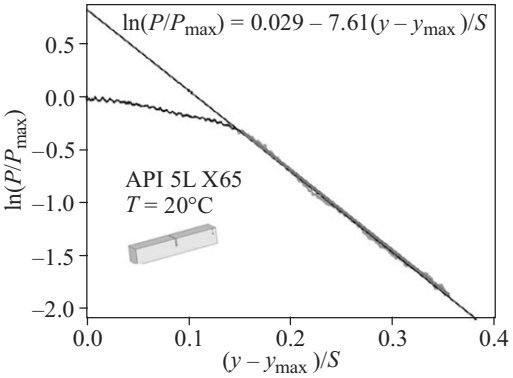


Fig. 8. Example of simplified single-specimen method (SSM) applied to a Charpy specimen made of X65 pipe steel

$d\alpha$, and the deflection y increases by dy. The derivative of the limit load is given by

$$dP_L = \frac{8AR_cBb}{S}db = \frac{8AR_cBb}{S}\left(-\frac{r^*b}{\tan(\Psi/2)}d\alpha\right) = \frac{8AR_cBb}{S}\left(-\frac{r^*b}{\tan(\Psi/2)}\frac{2dy}{S}\right) \quad (12)$$

with $db = -da$ and $d\alpha = 2dy/S$. By substituting da into (12), one gets

$$dP_L = -\frac{4r^*P_L}{S\tan(\Psi/2)}dy \quad (13)$$

by rearrangement

$$\frac{d\ln P_L}{dy} = -\frac{4r^*}{S\tan(\Psi/2)}. \quad (14)$$

The $\ln P_L$ versus $y - y_{max}/S$ curve may be used to evaluate Ψ, requiring values only for r^*. Constancy of the slope implies constancy of the CTOA

$$\psi(^\circ) = \frac{2.18}{\pi}\arctan\left(-\frac{4r^*}{d\ln P/dy)}\right). \quad (15)$$

An example of such an evaluation of CTOA from a Charpy test of X65 pipe steel is given in Fig. 8.

Moreover, this method is strongly dependent on the reliability of the limit bending load hypothesis. In addition, strain hardening is not taken into account. For this reason, Fiang et al. [22] evaluated the crack extension according to the procedure of the key-curve method, where load and displacement are related according to

$$\frac{PW}{b_0^2} = m\left(\frac{y}{W}\right)^n, \quad (16)$$

where W is the width, b_0 the initial ligament size, and m and n are constants. The key curve is analytically established by fitting the original relationship between the load P and displacement y on the prepeak part of the instrument curve. After obtaining the parameters m and n the amount of the crack extension is estimated at any displacement on the post-peak part of the force–displacement curve, as

Table 1

Mechanical properties of pipeline steel API 5L X65 at 20°C

Yield stress σ_y, MPa	465.5
Ultimate strength σ_{ul}, MPa	558.6
Elongation at failure A, %	10.94
Charpy energy K_{CV}, J	285.2
Fracture toughness K_{Ic}, MPa·m$^{1/2}$	280

$$\Delta a = W - \sqrt{\frac{PW^{n+1}}{my^n} + a_0}. \quad (17)$$

Combining (16) and (17),

$$\frac{\tan\Psi}{2} = -\frac{2r^*}{S}\frac{dy}{d\ln(W-a)}. \quad (18)$$

The $d\ln(W-a)$ versus $(y - y_{max}/S)$ curve may be used to evaluate Ψ, requiring values only for r^*

$$\frac{\tan\Psi}{2} = -2r^*\frac{d[(y-y_{max})/S]}{\Delta\ln(W-a_0-\Delta a)}. \quad (19)$$

2.3. CTOA value at stable crack growth for an X65 pipe steel

The investigated material is an API 5L X65 grade pipeline steel supplied as a seamless tube with a wall thickness equal to 19 mm and external diameter of 355 mm. The mechanical properties, measured at room temperature on three tensile test specimens in the circumferential direction, are given in Table 1.

Using a modified compact tension (MCT) specimen at room temperature, tests are performed to measure the value of the CTOA during crack extension. The design and dimensions of the test specimen are shown in Fig. 9. The study specimens were pre-cracked to provide an initial ratio of crack length to specimen width of $a/W = 0.4$ using a fatigue stress ratio $R = 0.1$. The sinusoidal loading oscillates at a frequency of 15 Hz and the maximum load is kept below 7.2 kN. According to ASTM E2472 [11] requirements,

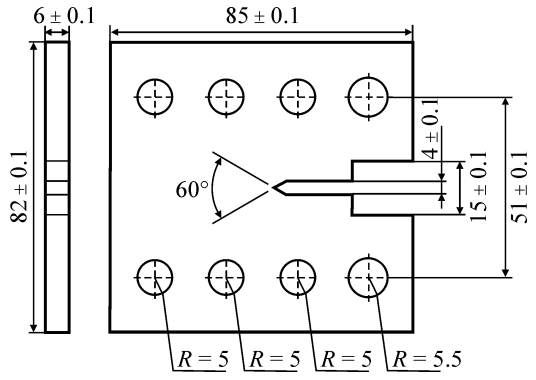


Fig. 9. Modified compact tension (MCT) specimen for determination of CTOA versus crack extension

Table 2

Values of $CTOA_c$ of API 5L X65 pipe steel obtained with three different methods

Method	DIC (MCT)	CNM (MCT)	SSM (Charpy)
Ψ_c	20.66°	24.68°	21.80°

the CTOA measurements were made at a distance behind the crack tip ranging between 0.5 and 1.5 mm. CTOA was determined using optical microscopy, with finite element fitting of the experimental load. In addition, it CTOA was also determined on a Charpy specimen using the simplified single-specimen method. Values obtained with the different are given in Table 2.

For all experimental tests, the CTOA versus crack extension behaviour consisted of an initially high CTOA region that quickly transitioned into a clearly constant CTOA region. The stable value of CTOA is called $CTOA_c$.

An average $CTOA_c$ is set as 20°. This value is compared with other values of $CTOA_c$ found in the literature (Table 3).

One notes that the values obtained are higher than other values found in the literature (Table 3). The confidence in the obtained value is given when examining Table 2, where three different methods give practically the same $CTOA_c$ value.

The MDCB specimen provides a longer stable crack extension in tension, and the long uncracked ligament combines with the large flat side-grooves (obtained with the addition of the loading plates) to allow a larger positive T stress ahead of the crack tip. This positive T stress is attested by the fact that the final fracture in the MDCB specimen always occurs after bifurcation. The MDCB specimen has loading characteristics similar to those of the compact C(T) specimen. This important positive T stress is not a realistic representation of the stress state of a gas transmission pipe which has higher negative T stress. In addition, the use of large flat side-grooves obtained in addition to the flank plates lead to a near plane strain situation, which adds a high lateral constraint effect, which also decreases the fracture resistance and therefore the CTOA values. It is now well known that fracture resistance decreases when the thickness increases. The fracture resistance is maximal for plane stress conditions and trends asymptotically to a minimum called K_{Ic} or J_{Ic} if the plane strain conditions are satisfied. The effect of thickness B on fracture is introduced by a "triaxial stress constraint" T_z. This parameter is defined as:

$$T_z = \frac{\sigma_{zz}}{\sigma_{yy} + \sigma_{xx}}. \quad (20)$$

For a straight through-thickness crack, which is a typical case of 3D cracks, y is the direction normal to the crack plane xOz. In an isotropic linear elastic cracked body, T_z ranges from 0 to N, $T_z = 0$ for the plane stress state, and $T_z = N$ for the plane strain state, where N is the strain hardening exponent of the Ramberg–Osgood strain–stress relationship. Values of T_z for different pipe thicknesses and same pipe diameter of 355 m) are reported in Table 4 and compared with plane stress or plane strain-stress states. One notes the low value of T_z for the M(CT) specimen used in this study.

A combined effect of constraint and thickness can explain the lower values of CTOA found in the literature.

Table 3

Values of $CTOA_c$ found in the literature and in the present study for API 5l X65 steel

References	Yield stress, MPa	$CTOA_c$	Specimen
[23]	447	8.10°	DWTT
[23]	529	14.20°	DWTT
[24]	543	11.61°	MDCB
Current study	465	20.00°	M(CT)
[25]	460	11.00°	MDCB
[25]	522	8.60°	MDCB

3. CTOA as a fracture resistance parameter

For the simulation of crack extension in a ductile material it is necessary to know the fracture resistance of the material. Several approaches are used, of which some are global and others are local. The impact fracture energy measured in Charpy or DWTT tests or obtained by static tests as the critical J energy parameter is considered as a global parameters that is constant during crack extension. The yield locus after damage or cohesive zone energy is a local criterion of this type. They are also considered as constant with crack extension. Use of the crack growth resistance curve (R-curve) and particularly the δ_R–Δa curve slope as the CTOA is another approach. In these approaches, CTOA can be assumed to be non-constant with crack extension.

Initially and particularly in standard methods for determining crack extension in pipes such as the BTCM [13],

Table 4

Triaxial stress constraint T_z values with pipe thickness for a pipe diameter of 355 mm

Wall thickness, mm	T_z
Plane stress	0.0000
6 (this study)	0.2040
10	0.2629
15	0.3109
19	0.3350
Plane strain	9.5200

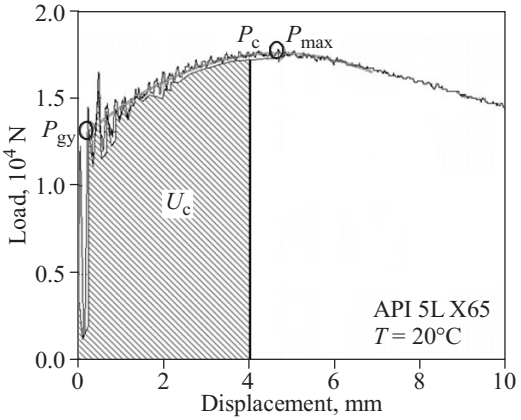


Fig. 10. Instrumented Charpy impact test. Definitions of load at general yielding, maximum load, critical load, and energy for fracture initiation U_i

HLP [14], and HLP-Sumitomo [26], fracture resistance is described as the specific fracture energy R_f obtained either from the Charpy-V energy or modified Charpy energy, or either from DWTT energy from standard or embrittled specimens. The specific fracture energy is the energy for fracture divided by the ligament area.

The specific fracture energy obtained from Charpy specimens consists of two parts: energy for crack initiation and energy for crack extension. The ratio of energy for crack extension over total energy decreases when the yield stress of the material decreases. Examination of an instrumented Charpy test on X65 pipe steel indicates the difficulty of using Charpy energy as fracture resistance to ductile crack extension.

A test campaign was conducted with an instrumented Charpy pendulum with an initial energy of 300 J and an impact rate of 5.5 ms^{-1}.

The acquisition of the results takes the form of voltage-time data $V_F = f(t)$. These curves show more or less light oscillations, resulting from the impact vibration, characterized by the loss of contact (hammer–specimen and/or anvil–specimen) as the peaks of inertia.

For ductile failure, the load increases to reach the point P_{gy} denoting the beginning of plastic flow of the ligament and the load reaches peak load at point P_{max}. Crack initiation occurs at the critical load P_c between the load at general yielding P_{gy} and maximum load (Fig. 10). The compliance changing rate (CCR) method [27] or a method proposed by Chaouadi [28] is used to determine the critical load. For API 5L X65 at 20°C, the ratio of energy for fracture initiation U_i to energy for fracture U_c is 21.3%. A comparison with the X52 pipe steel is made in Table 5 and indicates that this ratio decreases when the yield stress increases.

Table 5

Ratio of energy for fracture initiation to energy for fracture for X52 and X65 pipe steel

	Yield stress	U_i/U_c, %
X65	465	21.30
X52	436	26.54

The BTCM [13] is still used frequently today to predict ductile crack extension in pipes. Nevertheless, as higher-grade steels have been developed, it was found from full-scale tests that a multiplier was needed for the minimum Charpy arrest energy calculated from the BTCM. Several researchers have also suggested that a correction factor is needed for the Charpy energy when its value increases above a certain level. A correlation between Charpy-V energy K_{CV} and CTOA has been proposed by [29], where CTOA is in degrees and K_{CV} in joules

$$\Psi_c = 0.05K_{CV}. \quad (21)$$

In the HLP method [14], the pre-crack DWTT absorbed energy has been proposed as a better indicator to express resistance to fracture propagation, as a similar fracture surface to the running ductile fracture. Impact tests have been performed on a vertical hammer. Specimens have a length of 130 mm, a width of 20 mm, and a thickness of 10 mm. They are extracted from an API 5L X65 steel pipe with an outside diameter of 219.1 mm and a thickness of 12.7 mm.

The specimen has a V notch along the tangential direction with a depth a = 5 mm and a notch radius of 0.25 mm. The drop-weight apparatus is a floor-standing impact system designed to deliver 0.59–757 J or up to 1800 J with an optional high energy system. The specimen is submitted to vertical impact bending at a speed of 5.5 m/s.

Here the CCR method [27] is used to determine the fracture initiation. The rate of change in compliance $\Delta C/C$ is given by Eq. (22), where C is the current compliance and C_{el} is the elastic compliance:

$$\frac{\Delta C}{C} = \frac{C - C_{el}}{C}. \quad (22)$$

Figure 11 gives the registered load displacement diagram of a DWTT test on a flat specimen made in X65 pipe steel. For API 5L X65 at 20°C, the ratio of energy for fracture initiation to energy for fracture is 32.4%. The value of this

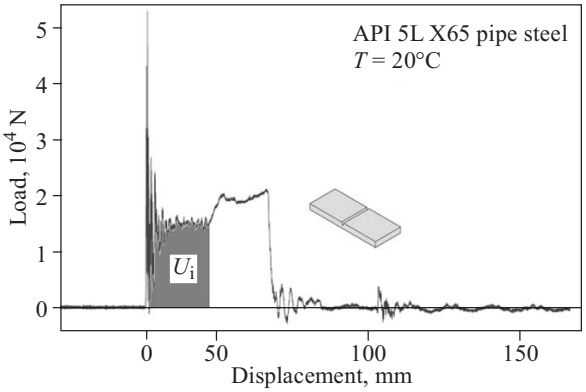


Fig. 11. Load displacement diagram of a DWTT test on a flat specimen made of API 5L X65 pipe steel

Table 6

Values of GTN constants for API 5L X65 pipe steel [33]

q_1	q_2	q_3	ε_N	f_0	f_N	f_i	f_c	l_y
1.5	1.0	4.0	0.3	$1.5\cdot10^{-4}$	$5\cdot10^{-4}$	0.02	0.04	0.25

ratio is higher than those obtained from the Charpy test and does not follow the argument in favour of DWTT energy used as fracture resistance for a running crack

To overcome the difficulty in using a fracture resistance parameter including the energy for fracture initiation, Demofonti et al. [15] proposed a method of subtracting energy for fracture initiation U_i by finding the difference between the fracture energies of two similar DWTT specimens but with different initial notch depths of $a_1 = 10$ mm and $a_2 = 38$ mm respectively. According to the limit load given by Eq. (11), the CTOA_c can be expressed with the propagation energy U_p:

$$\Psi_c = 2\arctan\frac{r^* U_p}{AR_c B(W-a_0)^2} \tag{23}$$

assuming that $\tan\Psi = \Psi$ for a small angle in rad unit, as expressed by the following equation:

$$\mathrm{CTOA}_c = \frac{[U_c/(B(W-a_1))]_{10} - [U_c/(B(W-a_2))]_{38}}{28AR_c}. \tag{24}$$

The Gurson–Tvergaard–Needleman (GTN) damage model of the yield locus considers that the yield locus Φ is affected by porosities which are created during the ductile fracture process. It is a function of hydrostatic pressure σ_h and the effective porosity f^*

$$\Phi = \frac{\sigma_{eq}}{R_c} + 2q_1 f^* \cosh\left[-q_2\left(\frac{3\sigma_h}{2R_c}\right)\right] - (1+q_3 f^{*2}). \tag{25}$$

Initially the material as a fraction of inclusion f_0 is considered. These inclusions are considered as voids. During the ductile fracture process, the size of pores increases and coalescence appears for the strain ε_N with a volume fraction f_N. These larger pores increase more rapidly and crack initiation occurs for the volume fraction f_i. Final fracture occurs for the volume fraction f_c

$$\begin{aligned} f^* &= f \quad \text{for} \quad f \le f_i, \\ f^* &= f_i + \frac{\overline{f}_c - f_i}{f_c - f_i}(f - f_i). \end{aligned} \tag{26}$$

After coalescence, the volume fraction is submitted to a linear acceleration governed by the parameter $\overline{f}_c$

$$\overline{f}_c = \frac{q_3 + \sqrt{q_1^2 - q_3}}{q_3}. \tag{27}$$

The GTN model needs eight constants. Values of these constants for API 5L X65 pipe steel are given in Table 6 and extracted from [30].

The great number of parameters and the difficulty of identifying them are the major handicap of this method,

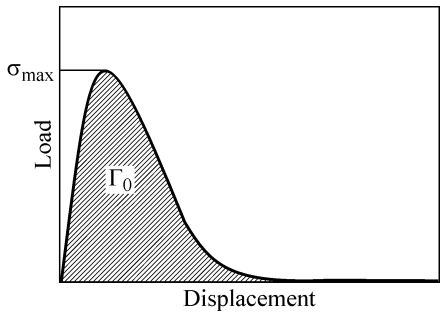


Fig. 12. Definitions of the cohesive zone model parameters

which requires tensile tests and observation with a scanning electron microscope. In [30], simulation of crack extension using the GTN model is replicated relatively simply, requiring no advanced meshing techniques. The element layer with a width equal to the parameter l_y was defined along the crack propagation path. The initiation and dynamic crack propagation are triggered once the critical crack length is reached. The crack propagation distance is limited to five times the outer diameter. The disadvantage of using local damage models for large-scale simulations is important. Due to this fine mesh resolution, the number of elements in the pipe model exceeds 10^6, resulting in the enormous CPU time.

Using the cohesive zone model (CZM), fracture extension is regarded as a gradual phenomenon in which the separation of the crack takes place across an extended crack tip or cohesive zone. The fracture resistance is simulated by cohesive tractions. As the surfaces separate, the opening stress first increases until a maximum σ_{max} is reached and then subsequently decreases to zero, which results in complete separation. The variation in traction versus displacement is plotted on a curve called the traction–displacement curve. The area under this curve is equal to the energy needed for separation Γ_0 (Fig. 12).

For an API 5L X65 steel pipe, Scheider et al. [30] proposed the values of σ_{max} and Γ_0 given in Table 7.

Simulations of ductile cracking with the CZM are generally performed using coarser mesh, and this reduces the number of elements. The criterion for crack extension is fulfilled when the energy of separation reaches the critical values. The model is sensitive to the shape of the traction–displacement curve. The two parameters of the model are obtained by fitting numerical results and cannot be obtained independently. This is a strong limitation of the validity of the method.

Table 7

Values of the parameters σ_{max} and Γ_0 of the cohesive zone model for API 5L X65

CZM parameters	σ_{max}, MPa	Γ_0, N/mm
API 5L X65	1375	900

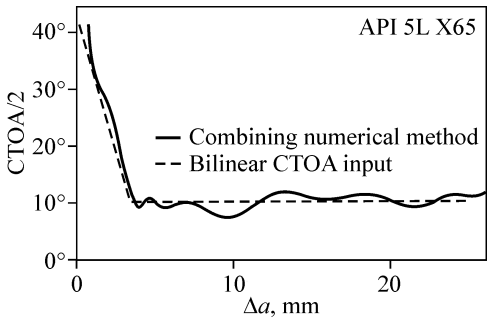


Fig. 13. Bilinear description of critical CTOA versus crack extension

The critical CTOA offers the possibility of describing stable crack extension with a single parameter Ψ_c obtained according to a standard test [11]. For a better agreement between the experimental and predicted curves, a bilinear form of CTOA should be used instead of the constant CTOA criterion (Fig. 13). Therefore the non-stable ductile crack extension can also be modelled. Non-stable crack extension affects few millimetres, while the stable one sometimes affects several metres.

The critical CTOA is sensitive to geometrical parameters such as thickness or ligament size and loading mode through constraints, but this is a general problem for all fracture criteria.

Table 8 gives a summary of different methods of modelling crack extension showing the number of parameters, advantages, and disadvantages. One notes that CTOA is an eligible one-parameter fracture resistance for ductile crack extension.

4. The use of the CTOA criterion to simulate ductile crack extension in a pipe submitted to internal pressure

The use of CTOA to model the ductile crack propagation of thin structures has been validated by several authors [31, 32]. Gullerud et al. [31] developed a 3D finite element model using the CTOA criterion to describe crack propagation in mode I of a thin aluminium plate. Hampton et al. [32] used the same criterion for the same purpose for thin plates and tubes made in 2219-T87 aluminium alloy.

To simulate crack propagation, the CTOA fracture criterion is introduced in a numerical model using the node release technique, as shown in Fig. 14.

The node release technique is based on the assumption that the crack growth is described by uncoupling nodes at the crack faces, whose acting tractions are reduced as far as the crack opens. When the CTOA reaches its critical value $(\Psi = \Psi_c)$, the representative node of the crack tip is released and a new position of the crack is deduced. Each propagation step corresponds to the size of a mesh element (see Fig. 2). In this method, crack evolution depends on the size of mesh elements around the crack tip, since it governs the amount of the crack advance. Moreover, the advancing process is not really continuous since a proper iteration scheme is necessary to accurately evaluate the dynamic crack growth during the integration time.

The method requires a priori knowledge of the crack propagation path. The crack propagation can be directly stimulated in a 2D ABAQUS model using the option "Debond" without any assumptions regarding material behaviour, loading, and boundaries. The meshing step is done with the linear elements CPE4 (plane strain) or CPS4 (plane stress). A user subroutine was developed to introduce CTOA in a 3D Abaqus model. The MPC (multi-point constraint) method has been used to elaborate this user subroutine.

The user subroutine allowed us to introduce a new fracture criterion. To simulate crack propagation by the node-release technique, it is necessary to change the boundary condition (crack surfaces) in each step of the computation. The implementation of the MPC method makes it possible to introduce the node release technique in the model simulation. This method requires a particular meshing (Fig. 15), with four nodes located in the same coordinates rather than the conventional meshing with one node at each element

Table 8

Different methods of modelling crack extension

	R curve	TCM	$CTOA_c$	Gurson	CZM
Number of parameters	COD or COD_5 versus crack extension	4, including fracture resistance	1	8	2
Advantages	Conventional *R* curve; easy and quick analytical or numerical assessment	Energy for initiation is included; ordinary ordinary FE method	Directly linked to crack extension	Linked with the micromechanisms; constraint effect taken into account	Simple model; ability to model branching crack
Disadvantages	Limited transferability	Fracture resistance difficult to define; transferability through geometrical parameters	Large scatter of CTOA values	Non-standard calibration; mesh-dependence; long computational time	Needs predefined crack path

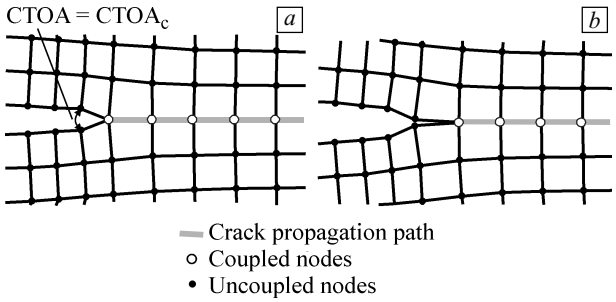


Fig. 14. Crack propagation according to the node release technique and the CTOA criterion in mode I and 2D: before (*a*) and after release (*b*)

corner. Nodes r, b, y, and p of the four elements R, B, Y, and P are coupled together, forcing their displacements to be the same

$$u_r = u_b = u_y = u_p. \quad (28)$$

To create a crack surface, these nodes have to be separated following the crack growth direction. The constraint equations are regenerated in each step of the computation to indicate one of the three possible directions of crack growth.

The simulation is performed on a pipe with an outer diameter of 393 mm, wall thickness of 19 mm, and length of 6 m. The studied pipe is made of API 5L X65 steel with a critical CTOA value of 20°. The computing phase begins by generating a 3D finite element implicit dynamic analysis. Because of the symmetry of the crack planes, only a quarter of the pipeline was analysed. A combined 3D-shell mesh was used to reduce the computing time. A total of 50976 eight-node hexahedral elements were generated along the crack path and combined with 6000 shell elements. Instantaneous internal pipe pressure was imposed along a certain distance behind the crack-tip node. This distance, where R and t are the outer radius and wall thickness, respectively, is given by the CZM [33].

The intensity of this pressure is given by the decompression wave. A simplified gas depressurization model is adopted in this work and assumes that the gas decompression depends only on time and distance from the crack tip. These assumptions are justified by the fact that crack propagation cannot outrun the decompression wave. This means that the crack tip is always present in the pipe section affected by the decompression process. Secondly, the expansion of ideal gas is isentropic, and the pipe is considered as a large pressure vessel with constant volume. The pressure drop ahead of the running crack tip is given by the following equation:

$$p(t) = p_0 \exp(kt), \quad (29)$$

where k is a constant, $k = -7.5\ s^{-1}$ [34] that can be related to the gas parameters and initial conditions of pressure and temperature.

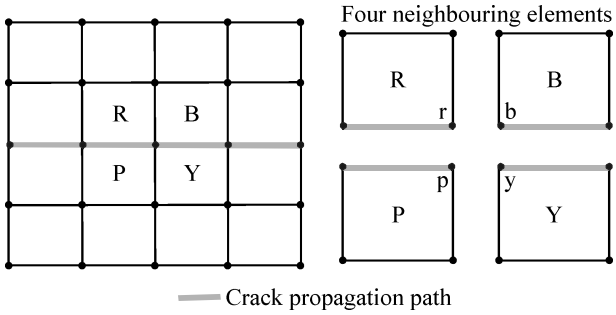


Fig. 15. Mesh with multinode construction

Mesh dependence was checked with three different 3D meshes. The results presented in Table 9 indicate that a good convergence can be obtained by observing a minimum level of mesh refinement. This level may be related to the definition of the CTOA and the maximum size of an element cannot exceed 1.5 mm.

Crack extension from an initial crack-like defect is computed using the described model. Running crack propagation along the tube consists of two stages: a boost phase, where the crack reaches its full velocity in a few milliseconds, followed by a steady stage at constant speed. The absence of a deceleration phase is explained by the absence of a pressure drop.

Figure 16 shows typical simulation results for two initial pressures $p_0 = 32$ and 40 MPa. One notes that the crack velocity increases with the initial pressure. Ten simulations were performed at different levels of pressure in the range of 25–60 MPa. The results indicate that the stationary crack velocity V_c [m/s] increases with initial pressure p_0 in megapascals according to

$$V_c = 290\left(\frac{p_0}{24} - 1\right)^{0.14}. \quad (30)$$

Crack extension at arrest is obtained from the graph of crack velocity versus half the crack extension, to take into account the symmetry of the problem. For the abovementioned conditions of geometry, material, and initial pressure, the numerical simulation gives a crack extension of 42 m, which is of the same order of magnitude as those obtained experimentally (Fig. 17).

Table 9

Influence of mesh refinement on crack velocity obtained by the node release technique

	Number of nodes	Number of elements	Element size, mm	Working time, h	Crack velocity, m/s
Mesh 1	48 196	36 181	3.0	32	266.85
Mesh 2	75 748	57 277	1.4	50	264.13
Mesh 3	237 717	189 085	0.7	210	260.89

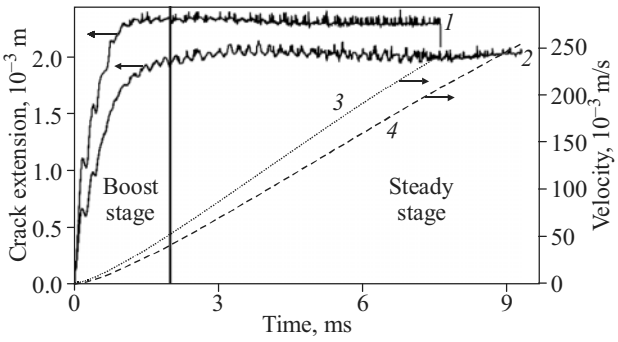


Fig. 16. Crack extension versus time simulation using CTOA ABAQUS user subroutine. Pipe pressure 32 (*1*, *3*) and 40 MPa (*2*, *4*)

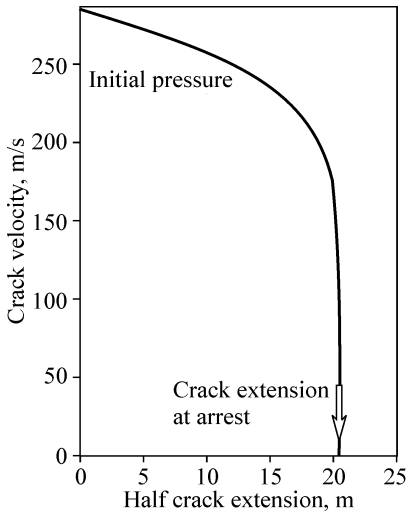


Fig. 17. Graph of crack velocity versus half of the crack extension; determination of crack extension at arrest, API5L X65 pipe steel, initial pressure p_0 = 45 MPa

5. Comparison with BTCM, HLP, and HLP-Sumitomo two-curve methods

On the assumption that the fracture toughness and driving force can be expressed by the crack propagation velocity and decompression wave speed, a minimum toughness to ensure ductile fracture arrest is required. This approach involves the superposition of two curves: the gas decompression wave speed and the ductile fracture propagation velocity characteristic, each as a function of the local gas pressure. For this reason, it is called the two-curves method (TCM). Several two-curve models for crack arrest have been introduced successively: the BTCM [13] and the HLP [14] and HLP-Sumitomo [26] methods.

In practice, the TCM approach consists of comparing the curves of the driving and resistance forces (Fig. 18, *a*–*c*). The relative positions of the two curves determine the potential for sustained fracture propagation or its arrest. If the two curves intersect as in Fig. 18, *c*, the fracture velocity is equal to the decompression wave speed and crack propagation will continue indefinitely at a constant speed. Non-intersection as in Fig. 18, *a* means that the decompression wave overruns the fracture propagation for all pressure levels and crack arrest occurs. Finally, the arrest/propagation boundary is represented by a tangent between the two curves and is associated with the minimum arrest toughness value (Fig. 18, *b*). All TCM models are based on the assumption that the decompression wave speed is uncoupled from the fracture velocity.

During the crack-propagation process, the gas escapes through the opening created in the wall of the pipe by the crack. Indeed, a decompression wave begins to propagate through the pipe at a speed of the order of 300 to 400 m/s. A number of models have been developed for predicting the gas decompression wave speed. Many of these assume a one-dimensional (along the pipe axis) and isentropic flow and use the finite difference method (FDM) or the method of characteristics (MOC).

BTCM is a model which assumes a one-dimensional, frictionless, isentropic, and homogeneous fluid and uses the Benedict–Webb–Rubin–Starling equation of state with modified constants to estimate the thermodynamic parameters during the isentropic decompression.

According to this one-dimensional flow model analysis and experimental results obtained from shock tube tests, the decompression pressure at the crack tip p_d is given by the relationship

$$\frac{p_d}{p_0} = \left(\frac{V_d}{6V_a} + \frac{5}{6} \right)^7, \qquad (31)$$

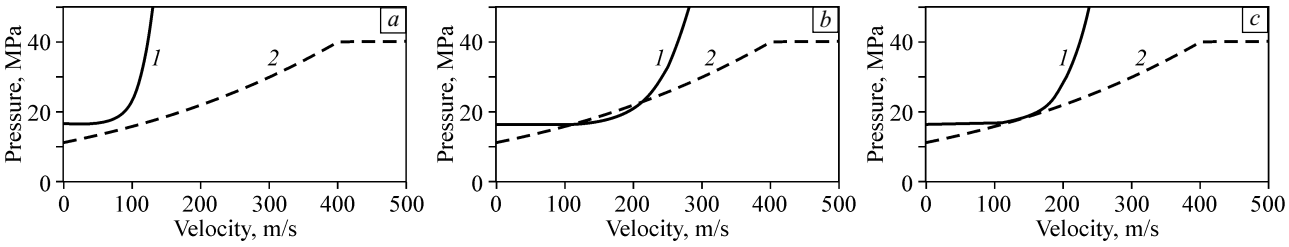


Fig. 18. Schema of the two-curve model for determining crack arrest or crack propagation: quick arrest (*a*), minimum arrest condition (*b*), propagation at 150 m/s (*c*). Fracture propagation (*1*) and gas decompression wave propagation (*2*)

Table 10

Analytic and numerical equations of crack velocity curves from the BTCM, HLP, HLP-Sumitomo, and CTOA models

Model	Analytic equation	Numerical equation for X65
BTCM	$V_c = 0.379\frac{\sigma_0}{\sqrt{R_f}}\left(\frac{p_d}{p_a}-1\right)^{1/6}$	$V_c = 90.2\left(\frac{p_0}{16.6\cdot10^6}-1\right)^{1/6}$
HLP	$V_c = 0.67\frac{\sigma_0}{\sqrt{R_f}}\left(\frac{p_d}{p_a}-1\right)^{0.393}$	$V_c = 211\left(\frac{p_0}{15.84\cdot10^6}-1\right)^{0.39}$
HLP-Sumitomo	$V_c = \alpha\frac{\sigma_0}{\sqrt{R_f}}\left(\frac{p_d}{p_a}-1\right)^{\beta}$	$V_c = 161\left(\frac{p_0}{15.86\cdot10^6}-1\right)^{0.023}$
CTOA		$V_c = 290\left(\frac{p_0}{24\cdot10^6}-1\right)^{0.14}$

where p_0 is the initial pressure, V_d is the decompression gas speed, and V_a is the acoustic speed.

It was proved by Battelle [13] that the ratio between the gas decompression wave and crack-propagation speed has a major role in the dynamics of crack growth. Indeed, if the crack propagates faster than the decompression wave, the crack tip is always loaded by the initial pressure p_0. Otherwise, the crack tip is progressively less and less loaded, up to crack arrest.

The BTCM is the oldest method and is still used frequently today to predict pressure at arrest and crack arrest length with the fracture resistance based on Charpy-V energy.

In the HLP method [14], the precrack DWTT absorbed energy has been proposed as a better indicator to express resistance to fracture propagation, and has a similar fracture surface of a running ductile fracture. The wall thickness of the DWTT specimen is set equal to the pipe thickness. The crack velocity curve $V_c = f(p_d)$ is given by Eq. (32)

$$V_c = 0.67\frac{\sigma_0}{\sqrt{R_f}}\left(\frac{p_d}{p_a}-1\right)^{0.393}. \quad (32)$$

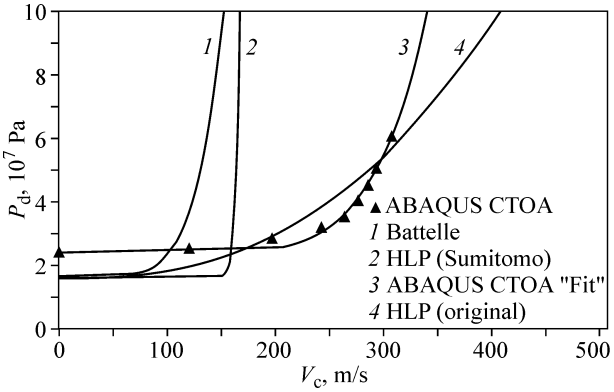


Fig. 19. Comparison of CTOA, BTCM, HLP, and HLP-Sumitomo TCMs for pipe with an outer diameter of D393 mm made of API 5L X65 pipe steel

The fracture resistance R_f is taken as the ratio of D_{DWTT} energy and the precracked test specimen area A_{DWTT}.

The new equation of the HLP-Sumitomo method [26] was developed in order to correct the arrest energy of a high strength pipeline, which is underestimated by the HLP and BTCM methods. The new crack velocity curve is given by Eq. (33)

$$V_c = \alpha\frac{\sigma_0}{\sqrt{R_f}}\left(\frac{p_d}{p_a}-1\right)^{\beta}, \quad (33)$$

$\alpha = 0.67[Dt/(D_0t_0)]^{1/4}\beta = 0.393(D/D_0)^{5/2}(t/t_0)^{-1/2}D_0$ and t_0 are reference dimensions, D_0 = 1219.2 mm and t_0 =18.3 mm.

Further, the BTCM and the HLP, HLP-Sumitomo, and CTOA TCMs are compared for the case of a pipe made of API 5L X65 pipe steel with the following data: K_{CV} = 260 J, D_{DWTT} = 280 J, and CTOA = 20°. The resulting crack velocity curves are reported in Table 10 and Fig. 19. Predictions of arrest pressure and crack extension are obtained and reported in Table 11.

These results indicate that HLP equation overestimated the crack propagation velocity and its extensions, which could be explained by the fact that the HLP model has not been validated for smaller pipe diameters. Nonetheless, this error is less severe than that obtained with the BTCM model,

Table 11

Predictions of arrest pressure and crack extension from BTCM, HLP, HLP-Sumitomo, and CTOA models for API 5L X65 pipe steel

Model	Arrest pressure, MPa	Crack extension at arrest, m
BTCM	16.60	23.8
HLP	15.84	40.7
HLP-Sumitomo	15.86	39.0
CTOA	23.00	32.1

where the crack velocity and crack extension are largely underestimated. The presented CTOA approach results shows a significant gap, of over 35%, in the prediction of the arrest pressure compared with those obtained by the BTCM and HLP method.

The HLP-Sumitomo version refers to pipe geometry (outer diameter and thickness) instead of the material mechanical intrinsic properties, which implies a deviation in smaller pipelines.

This drawback is not taken into consideration in the present CTOA approach, which probably represents the best way to predict crack arrest in pipelines.

6. Conclusion

CTOA is a measure of fracture toughness. More precisely, it expresses the fracture resistance to ductile crack extension in radians or degrees. These units come naturally from the definition of the CTOA as the angle between the crack faces of a growing crack or as the slope of the *R* curve $\delta_R = f(a)$. However a simple definition, its correct and simple definition exhibits some difficulty due to the irregular shape of the crack profile. The most appropriate methods follow the ASTM E2472-06e1 Standard [11] using an MDCB specimen and optical microscopy. An alternative method is to use the finite element method to fit experimental load–displacement diagrams mainly when the test temperature is low (it becomes difficult to carry out an optical examination of the specimen surface) or when the specimen is thick (due to the tunnelling effect).

Values of the CTOA are not intrinsic to materials. Like other measures of fracture toughness, it is sensitive to geometry and loading mode. This sensitivity can be described by a constraint parameter. For the thickness effect, the constraint parameter T_z is very appropriate.

CTOA is a good candidate to describe the fracture resistance of a ductile running crack. It represents only this resistance to crack extension and not a mixture of crack propagation and crack initiation energies. The use of this criterion requires a single parameter that can be obtained easily with a fracture test.

Comparison of the BTCM, HLP, HLP-Sumitomo and CTOA models to predict pressure and crack extension at arrest for API 5L X65 steel pipe indicates that the two first methods are conservative due to overestimation of the fracture resistance by taking into account the fracture initiation energy.

The HLP-Sumitomo and CTOA models gives close results in this particular case but the HLP-Sumitomo model depends on the pipe geometrical references (outer diameter and thickness) of an intrinsic material property. This implies a deviation of this concordance for smaller pipelines than the studied one.

However, the CTOA TCM model suffers from the sensitivity of CTOA to thickness. Recent results indicate that the influence of thickness on the arrest pressure of a pipe made of API 5L X65 steel (pipe with outer diameter D = 393 mm) in the range of 6–19 mm is small, being about 12% [35].

References

1. *Andersson H.* A finite element representation of stable crack growth // J. Mech. Phys. Solids. – 1973. – V. 21. – P. 337–356.
2. *Rice J.R., Sorensen E.P.* Continuing crack tip deformation and fracture for plane-strain crack growth in elastic-plastic solids // J. Mech. Phys. Solids. – 1978. – V. 26. – P. 163–186.
3. *Shih C.F., de Lorenzi H.G., Andrews W.R.* Studies on crack initiation and stable crack growth // ASTM STP. – 1979. – V. 668. – P. 65–120.
4. *Kanninen M.F., Rybicki E.F., Stonesifer R.B., Broek D., Rosenfield A.R., Nalin G.T.* Elastic-plastic fracture mechanics for two dimensional stable crack growth and instability problems // ASTM STP. – 1979. – V. 668. – P. 121–150.
5. *Newman J.C., Jr.* An elastic-plastic finite element analysis of crack initiation, stable crack growth, and instability // ASTM STP. – 1984. – V. 833. – P. 93–117.
6. *Brocks W., Yuan H.* Numerical Studies on Stable Crack Growth // Defect Assessment in Components Fundamentals and Applications. V. 9. – London: ESIS Publication, 1991. – P. 19–33.
7. *Luxmoore A., Light M.F., Evans W.T.* A comparison of energy release rates, the J-integral and crack tip displacements // Int. J. Fract. – 1977. – V. 13. – P. 257–259.
8. *de Koning A.U.* A Contribution to the Analysis of Slow Stable Crack Growth / National Aerospace Laboratory Report NLR MP75035U. – 1975.
9. *Reuter W.G., Graham S.M., Lloyd W.R., Williamson R.L.* Ability of Using Experimental Measurements of CTOD to Predict Crack Initiation for Structural Components // Defect Assessment in Components Fundamentals and Applications. V. 9. – London: ESIS Publication, 1991. – P. 175–188.
10. *Dawicke D.S., Sutton M.A.* CTOA and crack tunneling measurements in thin sheet 2024-T3 aluminum alloy // Exp. Mech. – 1994. – V. 34(4). – P. 357–368.
11. *ASTM* E2472-06e1. Standard Test Method for Determination of Resistance to Stable Crack Extension under Low-Constraint Conditions. – 2002.
12. *Zerbst U., Heinimann M., Donne C.D., Steglich D.* Fracture and damage mechanics modeling of thin-walled structures—an overview // Eng. Fract. Mech. – 2009. – V. 76. – P. 5–43.
13. *Maxey W.A.* Fracture Initiation, Propagation and Arrest // Proc. 5th Symp. on Line Pipe Research. PRCI Catalog No. L30174. – 1974. – P. J1–J31.
14. *Sugie E., Matsuoka M., Akiyama H., Mimura T., Kawaguchi Y.* A study of shear crack propagation in gas-pressurized pipelines // J. Press. Vess. Technol. – 1982. – V. 104(4). – P. 338–343.
15. *Demofonti G., Buzzichelli G., Venzi S., Kanninen M.* Step by Step Procedure for the Two Specimen CTOA Test // Pipeline Technology. V. II / Ed. by R. Denys. – Amsterdam: Elsevier, 1995. – P. 503–512.
16. *Demofonti G., Mannucci G., Hillenbrand H.G., Harris D.* Evaluation of X100 Steel Pipes for High Pressure Gas Transportation Pipelines by Full Scale Tests // Int. Pipeline Conf., Calgary, Canada, 2004.
17. *Lloyd W.R.* Microtopography for ductile fracture process characterization. Part 1: Theory and methodology // Eng. Fract. Mech. – 2003. – V. 70. – P. 387–401.
18. *Newman J.C., James M.A., Zerbst U.* A review of the CTOA/CTOD fracture criterion // Eng. Fract. Mech. – 2003. – V. 70. – P. 371–385.
19. *Heeerens J., Schödel M.* On the determination of crack tip opening angle, CTOA, using light microscopy and δ_5 measuring technique // Eng. Fract. Mech. – 2003. – V. 70. – P. 417–426.
20. *Xu S., Bouchard R., Tyson W.R.* Simplified single-specimen method for evaluating CTOA // Eng. Fract. Mech. – 2007. – V. 74. – P. 2459–2464.

21. *Martinelli A., Venzi S.* Tearing modulus, J-integral, CTOA and crack profile shape obtained from the load–displacement curve only // Eng. Fract. Mech. – 1996. – V. 53. – P. 263–277.
22. *Fang J., Zhang J., Wang L.* Evaluation of cracking behavior and critical CTOA values of pipeline steel from DWTT specimens // Eng. Fract. Mech. – 2014. – V. 124/125. – P. 18–29.
23. *O'Donoghue P.E., Kanninen M.F, Leung C.P., Demofonti G., Venzi S.* The development and validation of a dynamic fracture propagation model for gas transmission pipelines // Int. J. Press. Vess. Pip. – 1997. – V. 70. – P. 11–25.
24. *Darcis Ph.P., McCowan C.N., Windhoff H., McColskey J.D., Siewert T.A.* Crack tip opening angle optical measurement methods in five pipeline steels // Eng. Fract. Mech. – 2008. – V. 75. – P. 2453–2468.
25. *Amaro R.L., Sowards J.W., Drexler E.S., McColskey J.D., MacCowan C.* CTOA testing of pipe line steels using MDCB specimens // J. Pipe Eng. – 2013. – V. 3. – P. 199–216.
26. *Higuchi R., Makino H., Takeuchi I.* New Concept and Test Method on Running Ductile Fracture Arrest for High Pressure Gas Pipeline // 24th World Gas Conf., WGC 2009, Vol. 4, International Gas Union, Buenos Aires, Argentina. – 2009. – P. 2730–2737.
27. *Tronskar J.P., Mannan M.A., Lai M.O.* Measurement of fracture initiation toughness and crack resistance in instrumented Charpy impact testing // Eng. Fract. Mech. – 2002. – V. 69. – P. 321–338.
28. *Chaouadi R., Puzzolante J.L.* Loading rate effect on ductile crack resistance of steels using precracked Charpy specimens // Int. J. Press. Vess. Pip. – 2008. – V. 85. – P. 752–761.
29. *Cen Ch*. Characterization and Calculation of Fracture Toughness for High Grade Pipes: Thesis. – University of Alberta, 2013.
30. *Scheider I., Nonn A., Völling A., Mondry A., Kalwa C*. A damage mechanics based evaluation of dynamic fracture resistance in gas pipelines // Proc. Mater. Sci. – 2014. – V. 3. – P. 1956–1964.
31. *Gullerud A.S., Dodds R.H., Hampton R.W., Dawicke D.S.* Three-dimensional modeling of ductile crack growth in thin sheet metals: computational aspects and validation // Eng. Fract. Mech. – 1999. – V. 63(4). – P. 347–374.
32. *Hampton R.W., Nelson D*. Stable crack growth and instability prediction in thin plates and cylinders // Eng. Fract. Mech. – 2003. – V. 70 (3/4). – P. 469–491.
33. *Maxey W*. Dynamic Crack Propagation in Line Pipe // Analytical and Experimental Fracture Mechanics / Ed. by G.C. Sih, M. Mirabile. – 1981. – P. 109–123.
34. *Nordhagen H.O., Kragset S., Berstad T., Morin A., Dørumb C., Munkejord S.T.* A new coupled fluid-structure modelling methodology for running ductile fracture // Comput. Struct. – 2012. – V. 94/95. – P. 13–21.
35. *Ben Amara M., Pluvinage G., Capelle J., Azari Z.* Prediction of arrest pressure in pipe based on CTOA // J. Pipe Eng. (*in press*).

Поступила в редакцию
17.09.2015 г.

Сведения об авторах

Mohamed Ben Amara, PhD, LaBPS–ENIM, France, mohamed.ben.amara.enim@gmail.com
Guy Pluvinage, Emeritus Prof., FMC, France, pluvinage@cegetel.net
Julien Capelle, Dr. Ing., LaBPS–ENIM, France, capelle@enim.fr
Zitouni Azari, Prof., LaBPS–ENIM, France, azari@enim.fr